AGU ADVANCING EARTH AND SPACE SCIENCE

Water Resources Research

RESEARCH ARTICLE

10.1029/2022WR032736

Key Points:

- With careful design, solute tracer studies can be used to assess the fate of solute mass along flowpaths that would not normally be detected
- Extended mass recovery allows us to understand the formerly unknown fate of more than 26% of all lost tracer mass
- Accounting for mass recovery beyond the typical window of detection reduced inferred channel water turnover, changing interpreted spatial sources of gains

Supporting Information:

Supporting Information may be found in the online version of this article.

Correspondence to:

A. S. Ward,
adam.ward@oregonstate.edu

Citation:

Ward, A. S., Wondzell, S. M., Gooseff, M. N., Covino, T., Herzog, S., McGlynn, B., & Payn, R. A. (2023). Breaking the window of detection: Using multi-scale solute tracer studies to assess mass recovery at the detection limit. *Water Resources Research*, *59*, e2022WR032736. https://doi.org/10.1029/2022WR032736

Received 5 MAY 2022
Accepted 31 JAN 2023

Breaking the Window of Detection: Using Multi-Scale Solute Tracer Studies to Assess Mass Recovery at the Detection Limit

Adam S. Ward[1,2], Steven M. Wondzell[3], Michael N. Gooseff[4], Tim Covino[5], Skuyler Herzog[1,6], Brian McGlynn[7], and Robert A. Payn[8]

[1]O'Neill School of Public and Environmental Affairs, Indiana University, Bloomington, IN, USA, [2]Department of Biological and Ecological Engineering, Oregon State University, Corvallis, OR, USA, [3]Pacific Northwest Research Station, Forest Service, United States Department of Agriculture, Washington DC, WA, USA, [4]Institute of Arctic and Alpine Research, University of Colorado, Boulder, Boulder, CO, USA, [5]Department of Ecosystem Science and Sustainability, Colorado State University, Fort Collins, CO, USA, [6]Natural Resources Program, Oregon State University–Cascades, Bend, OR, USA, [7]Division of Earth and Ocean Science, Nicholas School of Environment, Duke University, Durham, NC, USA, [8]Department of Land Resources and Environmental Sciences, Montana State University, Bozeman, MT, USA

Abstract Stream solute tracers are commonly injected to assess transport and transformation in study reaches, but results are biased toward the shortest and fastest storage locations. While this bias has been understood for decades, the impact of an experimental constraint on our understanding has yet to be considered. Here, we ask how different our understanding of reach- and segment-scale transport would be if our empirical limits were extended. We demonstrate a novel approach to manipulate experimental conditions and observe mass that is stored at timescales beyond the traditional reach-scale window of detection. We are able to explain the fate of an average of 26% of solute tracer mass that would have been considered as "lost" in a traditional study design across our 14 replicates, extending our detection limits to characterize flowpaths that would have been previously unmeasured. We demonstrate how this formerly lost mass leads to predicting lower magnitudes of gross gains and losses in individual reaches, and ultimately show that the network turnover we infer from solute tracers represents an upper limit on actual, expected behavior. Finally, we review the evolution of tracer studies and their interpretation including this approach and provide a proposed future direction to extend empirical studies to not-before-seen timescales.

1. Introduction

The time that a parcel of water spends in various locations within a river corridor is a master variable that reflects the integrated effects of physical stores and fluxes and ultimately controls the biogeochemical processes and functions that are realized during transport. Empirical evidence of transit times in river corridors most commonly relies upon naturally occurring tracers to assess relatively long timescales (Cirpka et al., 2007; Gooseff et al., 2003; Lamontagne & Cook, 2007) and injected solute tracers for shorter timescales (Stream Solute Workshop, 1990; Ward et al., 2012). Studies using stream solute tracers are widespread in their application, but for more than 20 years have been known to be biased toward measuring the fastest portion of the transit time distribution, a limitation inherent to the method (J. W. Harvey et al., 1996; Wagner & Harvey, 1997). Despite the recognition of this limit, and the fact that the limitation is itself highly variable as a function of study design (e.g., Schmadel et al., 2016), hydrologists continue to conduct and interpret solute tracer studies. Any tracer that is released but not recovered (i.e., "lost") is attributed to flow that bypasses the monitoring location or transport along flowpaths longer than can be detected by monitoring equipment. In the latter case, such flowpaths could range in timescale from incrementally longer than what is detected to infinitely long. The inherent limits of tracer studies in streams define an arbitrary boundary that separates the tracer we are able to sense and interpret from the tracer we lose to the "black box" of longer timescales. While this demarcation is conceptually understood, we do not understand how this methodological threshold changes our understanding of transport in stream reaches (i.e., individual sections of river that are studied in an experiment, typically 10–100s of meters; Frissell et al., 1986). Moreover, when reaches are combined to represent segments (i.e., sections of a river that are comprised of multiple reaches, typically 100–1000s of meters; Frissell et al., 1986) it is unclear what impact—if any—the study limitations have on our understanding of transport in river corridors. Here, we ask how the well-documented and broadly acknowledged limits of solute tracer studies change our understanding at the reach- and segment-scales. In other words, if we manipulate the observational constraints of solute tracer studies to "peer into the black box", characterizing solute transport at timescales that have traditionally been lost to unknown fates, what would change about our understanding of transport in river corridors?

Stream tracer studies have been broadly successful in advancing our understanding of transport and fate in river corridors. Solute tracer studies underpin early work on mixing in streams and rivers (Fischer, 1979), and the reach-scale effects of transient storage both in hyporheic zones (Bencala, 1983; Bencala et al., 1984; Bencala & Walters, 1983; J. W. Harvey & Wagner, 2000; Jackman et al., 1984) and within stream channels (Briggs et al., 2009; Jackson et al., 2012, 2013; Ward et al., 2018). Indeed, tracer studies are a critical component of our ability to predict the fate of nutrients (Alexander et al., 2009; J. Harvey et al., 2019; Mulholland et al., 2008; Newbold et al., 1981; Tank et al., 2008), emerging contaminants (Guillet et al., 2019; Keefe et al., 2004; Lange et al., 2011), heavy metals (Fuller & Harvey, 2000; J. W. Harvey & Fuller, 1998; Larson et al., 2013), and more broadly to study timescales of storage in river corridors (Haggerty et al., 2002; Ward, Kurz, et al., 2019; Worman & Wachniew, 2007). Tracer studies have also been used to assess the impact of dynamic flow regimes (Karwan & Saiers, 2009; Ward, Gooseff, et al., 2013, Ward, Kurz, et al., 2019) and restoration (Klocker et al., 2009; Knust et al., 2009; Ward et al., 2018) on reach- and segment-scale functions. Despite their widespread use and interpretation for a host of applications, all solute tracer studies are limited by their "window of detection" (WoD), the longest temporal scale of flowpath that contributes to a measurable concentration in the stream channel (J. W. Harvey et al., 1996; Wagner & Harvey, 1997; N.M. Schmadel et al., 2013) (flowpaths A and B; Figure 1). Precisely defined, the WoD represents the longest elapsed timescale from the solute tracer release to the last recovery of solute tracer mass that is discernible from background at the downstream end of the study reach. Solute tracer that does not return to the stream to be observed, either due to flowpath geometry (flowpaths C, D; Figure 1), timescale (flowpaths E, F, where flowpaths do return to the study reach but the timescales are sufficiently long that concentrations are below the detection limit of instrumentation; Figure 1), or both (flowpath G, Figure 1) are ultimately lost to unknown fates, limiting interpretations to a subset of the known, multi-scale flowpaths that exist (Herzog et al., 2019; Toth, 1962; Tóth, 1963).

While the known limitations and biases of stream solute tracers have been understood for more than 25 years, it remains unknown if and how this limitation may actually bias our understanding of transport. These "lost" timescales and flowpaths are understood to be relevant for biogeochemical functions, contaminant legacies, and ultimately for complete description of transit time distributions. Consequently scientists have developed strategies to extrapolate behavior from observed to "lost" timescales (e.g., Drummond et al., 2012; Harman et al., 2016) to estimate the fate of "lost" tracer, but these rely upon assumptions and generally lack empirical validation. Flowpaths E and F (Figure 1) represent the detection limits that Drummond et al. (2012) explored—the tracer mass does return within the study reach (vs. flowpaths D and G, which are geometrically bypassing the sensor), but at such low concentrations that it cannot be differentiated from background due to detection limits. Such approaches broadly extrapolate observed data to timescales beyond the WoD, assigning monotonically decreasing probabilities as timescales extend. Put plainly, the most likely assumed fate for mass that is "lost" during an injection is to travel along flowpaths with timescales incrementally longer than the WoD. The next most likely fate is to travel along an incrementally longer flowpath, and so on (noting that here and throughout "longer" refers strictly to storage timescales). This conceptualization is consistent with empirical observations that targeted extremely long tailing (Haggerty et al., 2002; Ninnemann, 2005) and methods used to extend the tails of solute tracer data (Drummond et al., 2012). This is also consistent with age-of-water approaches to stream tracer transport, where gamma distributions have successfully represented monotonically decreasing contributions of older water to stream discharge (e.g., StorAge Selection; Harman et al., 2016; Ward, Kurz, et al., 2019; Ward, Wondzell, et al., 2019). Taken together, both our empirical studies, strategies to correct empirical data for known limitations, and process-agnostic approaches to solute tracers all predict that an incremental extension of the WoD should yield the most significant change in the observed in-stream breakthrough curve and subsequent interpretations, with decreasing impact as the WoD was further extended. Importantly, while the above strategies exist as a basis to extrapolate beyond observations, no empirical evidence exists to document that they are appropriate in describing the fate of tracer mass beyond the WoD.

The WoD is perhaps the most critical variable in our interpretation of solute tracer studies at individual reaches and our extrapolation to the segment and network scales. The WoD defines a fundamental partitioning of tracer mass into two categories: recovered and lost mass. The mass that was recovered within the WoD is interpreted using time series analyses to infer a host of transport and transient storage processes (e.g., Covino et al., 2010; J. W. Harvey & Wagner, 2000; Newbold et al., 1981; Stream Solute Workshop, 1990). The fate of mass along all

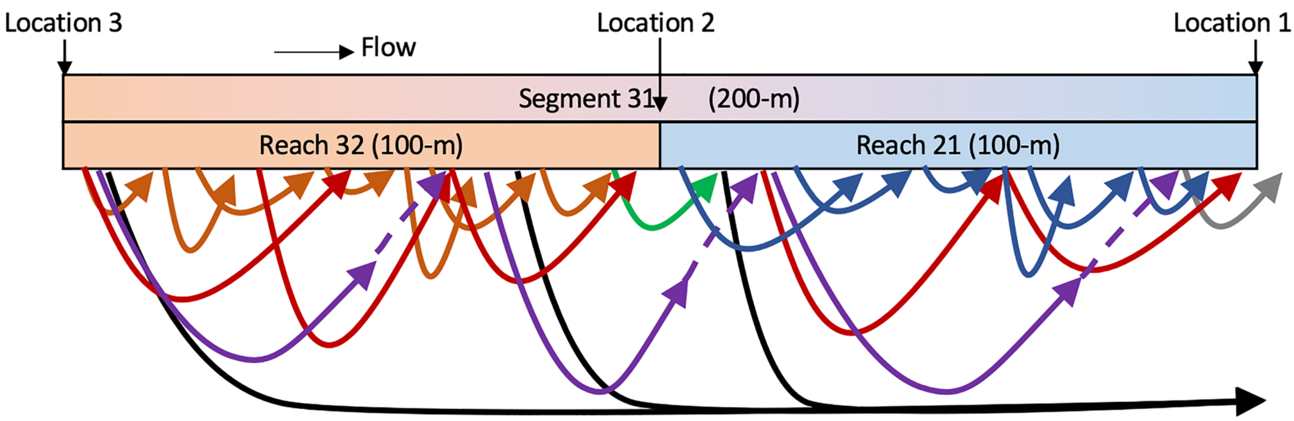

		Key Feature(s)	Observable for…			Mass loss observed in…		
			Reach 32	Reach 21	Segment 31	Reach 32	Reach 21	Segment 31
A		$\tau \leq WoD_{32}$	Y	--	Y	Y	--	Y
B		$\tau \leq WoD_{21}$	--	Y	Y	--	Y	Y
C		$\tau \leq WoD_{32}$	N	--	Y	Y	--	N
D		$\tau \leq WoD_{21}$	--	N	N	--	Y	Y
E		$WoD_{32} < \tau \leq WoD_{31}$ $WoD_{21} < \tau \leq WoD_{31}$	N	N	Y	Y	Y	N
F		$WoD_{31} < \tau$ Geometry Returns	N	N	N	Y	Y	Y
G		Geometry Bypasses	N	N	N	Y	Y	Y

Figure 1. Consider two contiguous, 100-m study reaches (reaches 32 and 21, respectively spanning from locations 3 to 2 and 2 to 1), where a solute tracer is injected at the upstream end of each reach. Seven distinct fates for solute tracer can be defined, including (a) tracer released to study segment 32 that returns to the stream within the window of detection (WoD) for that reach; (b) tracer released to study segment 21 that returns to the stream within the WoD for that reach; (c) tracer released to study reach 32 that bypasses the downstream end of that study reach due to flowpath geometry; (d) tracer released to study reach 21 that bypasses the downstream end of that study reach due to flowpath geometry; (e) tracer released to study either reach 32 or 21 transported along flowpaths that are too long to return within the WoD for the shorter segments, but which are short enough to return within the WoD for the combined segment 31; (f) tracer released that is transported along flowpaths too long in its transport timescale to return within the WoD for the combined segment 31, but whose geometry would eventually return within the study reach and would be detectable with increased observational sensitivity; or (g) flowpaths whose timescales and geometries exceed detection with the study segment, commonly "regional" flowpaths. Flowpath type E are the primary contributors to marginal mass recovery that is achieved when the WoD can be extended. The combination of reaches 32 and 21 is a 200-m segment spanning from locations 3 to 1, hereafter segment 31, which can also be studied.

other flowpaths and timescales beyond the WoD is ultimately unknown, but the magnitude of mass loss is used to interpret reach-scale water balances though gross gains and losses of channel water within a study reach (i.e., channel water balance; Payn et al., 2009), which themselves form the basis of how we predict channel water turnover along segments and river networks (Covino et al., 2011; Mallard et al., 2014). Critical to these analyses are the magnitude of mass that is ultimately lost, but that partitioning is known to be a function of study design itself (Schmadel et al., 2016), ultimately reflecting the WoD for the empirical studies. In this framework, increased mass recovery due to an extended WoD would decrease mass loss, consequently reducing magnitudes of gross gains and losses, ultimately reducing inferred channel turnover.

While the WoD is a well-known limitation of stream solute tracers, it has traditionally been accepted as a methodological limitation, either described post-hoc or as a basis to standardize experimental designs (e.g., Ward et al., 2018; Ward, Kurz, et al., 2019). Here, we posit that manipulation of the WoD through experimental design may be used to our advantage, specifically enabling us to assess solute transport that is just beyond the WoD for a common study, assessing the marginal gains in mass recovery—and understanding—associated with solute tracer mass that is just beyond our detection limits. In this study, we assess the influence of flowpaths that are incrementally longer than the WoD for a study reach by comparing the results of stream solute tracer tests in shorter reaches nested within longer reaches of the same stream. By doing so, we provide the first empirical test of the expectation that much of the lost tracer mass is being transported along flowpaths that are marginally longer than the WoD (Drummond et al., 2012; Harman et al., 2016). We term the added mass that is recovered when the WoD is experimentally extended "marginal mass recovery". Specific objectives of this study include: (a) empirical documentation of "marginal mass recovery" in a series of study reaches; (b) assessment of how marginal mass recovery changes interpreted reach-scale channel water balance; and (c) assessment of how marginal mass recovery changes our interpretation of segment-scale turnover. To achieve these objectives, we evaluate a series of solute tracer experiments conducted in the same study location, either as two sequential 100-m reaches combined to represent a single 200-m segment (hereafter 2 × 100-m) or as a single 200-m reach. We derive an "extended" mass balance (details in Supporting Information S1) that accounts for marginal mass recovery and demonstrate the change in interpretation that results from convolving these observations along a river segment. Finally, we address the crux of what is to be done with empirically imperfect data and their application to process understanding and scaling of findings.

2. Methods

2.1. Study Site and Field Experiment

Stringer Creek is a second-order stream in the Tenderfoot Creek Experimental Forest in the Little Belt Range of the Rocky Mountains in Montana, United States. The stream drains about 5.5 km^2 of primarily forested land. The valley is underlain by granite-gneiss bedrock along the lower 1600-m of the study, while upper reaches are underlain by sandstone bedrock. The upper valley has a generally wider valley floor, lower-relief hillslope, and flatter longitudinal slope than the lower valley. Additional site characteristics can be found in several prior studies (Kelleher et al., 2013; Patil et al., 2013; Payn et al., 2009; Ward, Payn, et al., 2013; Ward et al., 2016).

Our study design divided the river corridor into a series of contiguous 200-m segments. Each 200-m segment was studied with a series of three instantaneous solute tracer releases of known masses of sodium chloride at locations 1, 2, and 3 in that order (Figure 2a). Fluid conductivity was monitored at each location for the duration of the study, beginning before the first injection and ending after the upstream-most injection had passed the downstream-most logger. This scheme enabled us to study the segment as two independent 100-m reaches (hereafter reach 32 and 21, as they span from location 3 to 2 and 2 to 1, respectively), or a single 200-m segment (i.e., reach 31, spanning from location 3 to location 1). Briefly, solute tracer concentrations were background corrected using pre-release concentrations, converted from fluid conductivity to tracer mass using a calibration curve constructed from water at the field site, and clipped to isolate the tracer signal from background using visual inspection of the breakthrough curves. The data set here exactly matches that previously analyzed and published with no changes to the methodology nor QA/QC from those studies (see additional detail in Kelleher et al., 2013; Patil et al., 2013; Payn et al., 2009; Ward, Payn, et al., 2013; Ward et al., 2016). Notably, the data set has been independently analyzed as both 100-m and 200-m reaches, but the two have yet to be quantitatively compared to learn from deviations between the length scales and WoDs. In all cases, the analysis assumes steady-state discharge for each experiment conducted.

2.2. Analysis of Lost Solute Tracer Mass

2.2.1. Channel Water Balance for Individual Study Reaches

Discharge at each location was calculated by dilution gauging as:

$$Q_X = \frac{M_X}{\int_{t=0}^{t=\infty} C_{XX}(t)dt} \quad (1)$$

where X denotes the location number (e.g., M_3 is the mass released at location 3), $C_{XX}(t)$ is the observed in-stream tracer concentration at location X (g m^{-3}), M_X is the injected solute tracer mass at each location (g), and t is time (s). The tracer releases at points 2 and 3 are also recorded as they pass the downstream loggers, yielding in-stream concentration time series $C_{21}(t)$, $C_{32}(t)$, and $C_{31}(t)$, where C_{XY} denotes an injection from location X observed

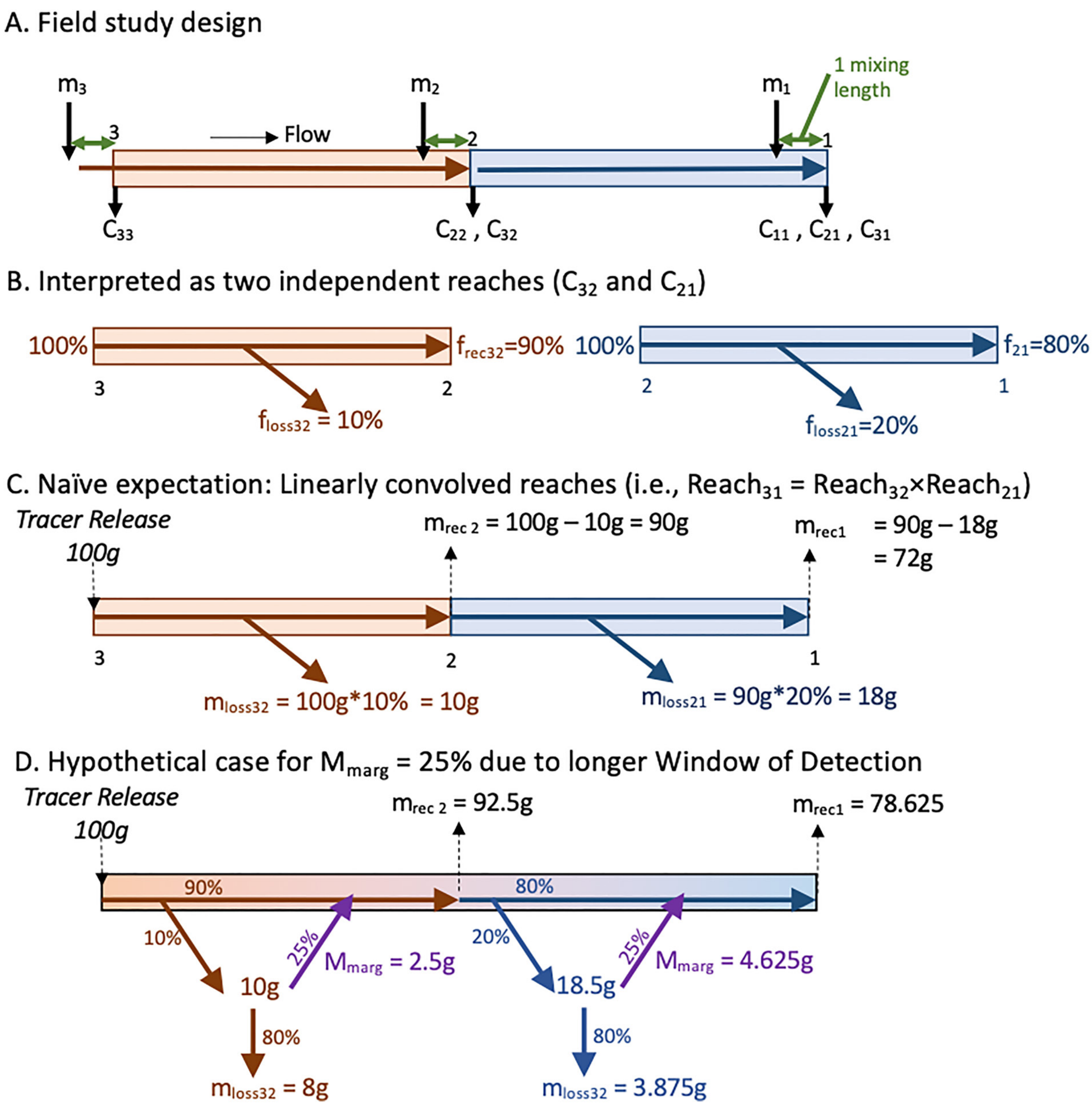

Figure 2. (a) Field study design showing tracer mass releases (m_X) and observed in-stream solute tracer timeseries (C_{XY}), where X is the release location and Y is the observation location. Note that locations 3, 2, and 1 refer to the up- and downstream ends of the orange and blue reaches depicted in panels A through C, where location 2 is both the upstream end of the blue reach and the downstream end of the orange reach. (b) Partitioning of recovered and lost solute tracer mass for two reaches interpreted independently. (c) Mass losses and recovery for a hypothetical 100-g solute tracer release at the upstream end of the study site, assuming the two 100-m reaches act on the input in series, forming a segment. (d) Mass losses and recovery for a hypothetical 100-g solute tracer release at the upstream end of the study site, assuming that the extended window of detection for a longer study reach yields 25% more mass recovery.

in-stream at location Y. We use the subscript XY to indicate a tracer release at location X observed at location Y for all variables. The mass recovered at any location can be calculated as:

$$M_{recXY} = Q_Y \int_{t=0}^{t=\infty} C_{XY}(t)dt. \tag{2}$$

Mass recovery can also be expressed as a fraction of input mass (f_{XY}) as:

$$f_{recXY} = \frac{M_{recXY}}{M_X}. \tag{3}$$

Total and fractional mass losses (M_{LOSSXY} and f_{lossXY}) can also be calculated as:

$$M_{LOSSXY} = M_X - M_{recXY} \tag{4}$$

and

$$f_{lossXY} = 1 - f_{recXY} \tag{5}$$

Payn et al. (2009) provide a framework to interpret tracer mass losses and calculate reach-scale gross gains (Q_{GAIN}) and gross losses (Q_{LOSS}). Briefly, gross losses of stream water are calculated by considering either gain-before-loss (i.e., maximum dilution before loss, subscript $_{MAX}$):

$$Q_{LOSS,MAX} = \frac{M_{LOSS,XY}}{\int_{t=0}^{t=\infty} C_{XX}(t)dt} \tag{6}$$

or loss-before-gain (i.e., minimum dilution before loss, subscript $_{MIN}$):

$$Q_{LOSS,MIN} = \frac{M_{LOSS,XY}}{\int_{t=0}^{t=\infty} C_{XY}(t)dt} \tag{7}$$

where M_{LOSS} is the mass loss along a study reach for an injection at location X observed in-stream at location Y. Next, the net change in discharge (ΔQ) can be calculated as:

$$\Delta Q = Q_Y - Q_X \tag{8}$$

Finally, knowledge of the net change in discharge and the gross losses can be used to calculate gross gains as:

$$Q_{GAIN,MAX} = \Delta Q - Q_{LOSS,MAX} \tag{9}$$

and

$$Q_{GAIN,MIN} = \Delta Q - Q_{LOSS,MIN} \tag{10}$$

In this study we proceed with interpretation of the loss-before-gain assumption, which assumes the minimum turnover of stream water caused by gross gains and losses along the study reach (after Covino et al., 2011; Ward, Wondzell, et al., 2019).

2.2.2. Network Turnover Analysis of the Study Segment

Covino et al. (2011) extended the interpretation of segment-scale channel water balances to river networks, developing a method to interpret network turnover. Briefly, the discharge in a downstream segment i can be calculated as:

$$Q_i = Q_{i-1} + Q_{GAIN,i} - Q_{LOSS,i} \tag{11}$$

where the subscript i denotes the values at an individual reach being analyzed and $i-1$ the upstream reach. The simultaneous gain and loss of water is assumed to remove water from all upstream segments equally, causing a volume-weighted replacement of upstream water with newly inflowing water. This is calculated as:

$$Q_{i,j} = Q_{i-1,j} \frac{Q_i - Q_{GAIN,i}}{Q_i} \tag{12}$$

where $Q_{i,j}$ is the discharge in segment i contributed by an upstream segment j, $Q_{i-1,j}$ is the stream water contribution to segment $i-1$ that entered in segment j, and the fractional term is the proportional contribution to Q_i from all upstream segments. For clarify, the subscripts X and Y are used to refer to analysis of individual reach-scale experiments while i and j are used when aggregating reach-scale results (from Section 2.2.1) to represent turnover at larger scales (i.e., segments; this section). This calculation can be completed sequentially from the headwaters to downstream end of the study segment. The result is an apportionment of the discharge in each study segment to the location(s) where that water last entered the stream channel.

2.3. Analysis of Marginal Mass Recovery

If the two 100-m study reaches are assumed to act independently and are combined in series to represent the single 200-m segment (Figure 2c), the mass recovered from the combined segment is calculated as the effect of the two segments acting on the upstream input in series:

$$M_{rec31,expected} = M_3 f_{rec32} f_{rec21} \tag{13}$$

where $M_{rec31,expected}$ is the expected mass recovery from a slug at location 3 observed at location 1 based on the linear convolution of the sub-segments. However, in practice this linear combination of segments may not be observed. Instead, studying a longer reach is expected to extend the WoD and allow increased mass recovery (i.e., $M_{rec31extended} > M_{rec31}$, compare Figures 2c and 2d). We term the extra mass recovered in the longer study segment the marginal mass recovery (M_{marg}), calculated as:

$$M_{marg} = M_{rec31,extended} - M_{rec31} \tag{14}$$

Conceptually, M_{marg} represents mass that was stored along flowpaths that were longer than could be detected in the observed C_{21} or C_{32} but short enough to return to the stream and contribute to C_{31} (i.e., flowpath E in Figure 1) or flow that bypassed the sensor at location 2 (i.e., flowpath C in Figure 1). Put another way, the timescales of intermediate storage (t_{int}) may be expressed as:

$$(t_{21}, t_{32}) < t_{int} < t_{31} \tag{15}$$

where t_{XY} represents the WoD for an injection at location X observed at location Y. While some marginal mass recovery is associated with flow that bypassed location 2 in the subsurface and returned to the stream (flowpath C in Figure 1), we assume this mass is negligible compared to the return of longer flowpaths along the entirety of the segment. The mass balance for the system of segments (Figure 2) can be written as:

$$M_3 = M_{rec31} + M_{loss32} + M_{loss21} \tag{16}$$

where M_3 is the mass input for the upstream-most injection. Calculations of masses for each individual segment and associated flowpaths are detailed in the supplement to this study. Briefly, we considered each 100-m reach to have some intermediate scale mass recovery, which would be observable when studying the larger 200-m reach. Thus, we have modified the 200-m mass balance to account for that added recovery. Mass losses from the shorter segments can be calculated as:

$$M_{loss32} = M_3(1 - f_{rec32})(1 - f_{int32}) \tag{17}$$

and

$$M_{loss21} = M_3[f_{rec32} + (1 - f_{rec32}) f_{int32}](1 - f_{rec21})(1 - f_{int21}) \tag{18}$$

Input mass (M_3) and recovered mass (M_{rec31}) are related by:

$$M_{rec31} = M_3[f_{rec32} + (1 - f_{rec32}) f_{int32}][f_{rec21} + (1 - f_{rec21}) f_{int21}]. \tag{19}$$

Based on the experimental design (Figure 2a), values are known for M_3, M_{rec31}, f_{rec32}, and f_{rec21}. The unknowns in the system are f_{int32} and f_{int21} which partition segment-by-segment losses into M_{marg} and M_{loss} for each study segment. For example, f_{int32} is the fraction of mass in segment 32 that is transported along intermediate-scale flowpaths that will not be recovered in studying segment 32 but will be recovered in studying segment 31 due to the longer WoD. We proceed with the assumption that mass beyond the WoD in the two 100-m study segments is equally likely to return within the WoD for the combined, longer segment (i.e., $f_{int32} = f_{int21}$). Finally, the mass balances for the individual and combined releases can be combined to yield an analytical solution for the system.

With the marginal mass recovery calculated, we next calculate an "extended" mass recovery. This "extended" recovery considers how the 100-m segment would be expected to behave if the WoD were extended to that of the 200-m segment. In other words, this step extends the empirical 100-m data to its expected, marginally longer behavior, accounting for the mass actually recovered (e.g., M_{rec21}) and the marginal mass recovery (e.g., M_{marg21}).

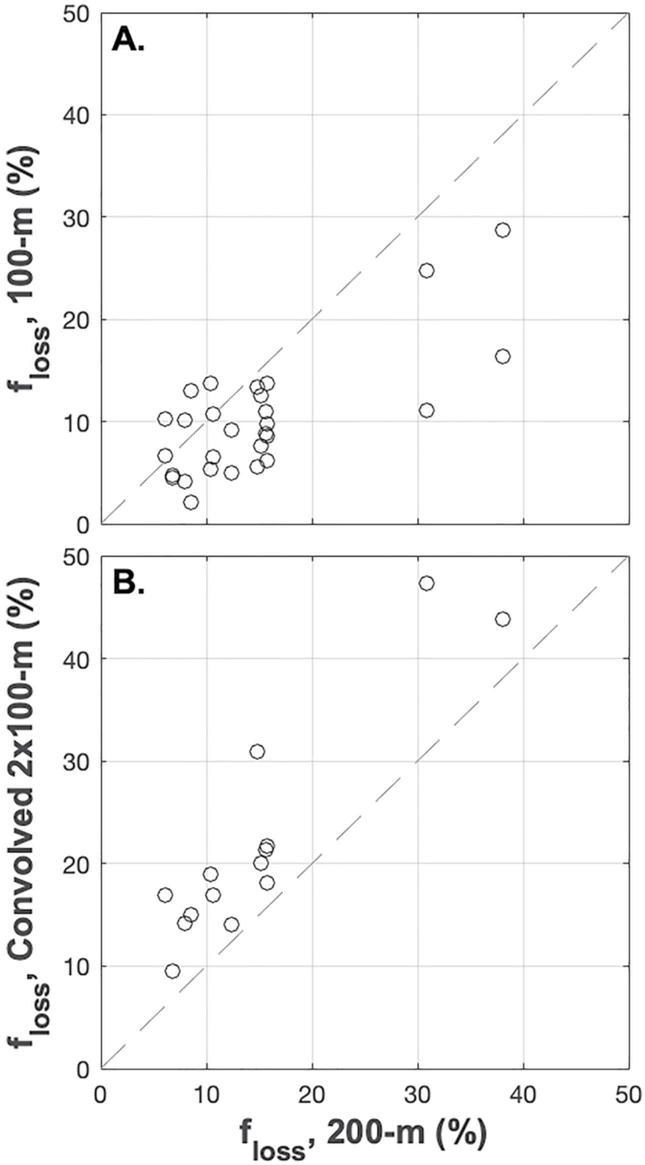

Figure 3. Comparison of the fraction of injected mass loss (f_{loss}) observed for 200-m study reaches (x-axis) in comparison to the same study reach studied as two 100-m reaches considered (a) individually, and (b) convolved in series as a segment. The convolution of two 100-m reaches to represent the 200-m overpredicts mass loss in all 14 replicates (i.e., more mass is recovered for the 200-m empirical study that would be expected). This systematic overprediction of losses is the result of marginal mass recovery in the 200-m reach.

Put another way, we can estimate the mass that would have been recovered for a marginally longer WoD in each 100-m segment as:

$$M_{rec21,extended} = M_{rec21} + M_{marg21} \tag{20}$$

$$M_{rec32,extended} = M_{rec32} + M_{marg32} \tag{21}$$

where $M_{recXY,extended}$ represents the mass recovery in segment XY that would be realized if the 100-m study had the WoD associated with the 200-m study. In turn, analysis of mass losses, channel water balance, and turnover calculations can all be updated using these extended values (i.e., analysis using Equations 4–12 replicated with the extended values).

3. Results

3.1. Marginal Mass Recovery and Channel Water Balance

The fraction of tracer mass loss in 200-m reaches is generally greater in magnitude than their component 100-m reaches (Figure 3a). However, total mass loss for the convolved 2 × 100-m case is always greater than the observed mass loss in each of the 200-m segments (Figure 3b). This increased mass recovery indicates some mass that was lost from the 100-m studies was recovered in the 200-m study with its longer WoD, confirming the presence of marginal mass recovery, M_{marg}. We found an average of 26.2% of mass presumed to be lost from the 100-m studies was ultimately recovered in the 200-m study segment (range 6.5%–63.1%, median 20.7%, standard deviation 17.2%; Figure 4a). These marginal recoveries represent an average of 4.3% of total tracer mass (range 1.3%–10.1%, median 3.4%, standard deviation 2.6%; Figure 4a) recovered in the 200-m studies that was lost in the 2 × 100-m interpretation. Increased mass recovery yields decreased magnitudes of gross gains and losses for each of the 200-m reaches considered (Figure 4b). Additionally, gross gains and losses for the extended 100-m reaches are always lower in magnitude than their empirically observed counterparts, as expected for $M_{marg} > 0$ (Figure 4c). Finally, to confirm these finding were not specific to the flow condition studied we also analyzed three comparable data sets from the same study site under different discharges (presented in Kelleher et al., 2013; Patil et al., 2013; Payn et al., 2009; Ward, Payn, et al., 2013; Ward et al., 2016). Increased window of detection for 200-m reaches compared to 100-m reaches was documented for more than 96% of experiments in the larger data set (Figure S2 in Supporting Information S1). Similarly, marginal mass recovery was documented for 75% of cases presented in the larger data set (Payn & Ward, 2022; Figure S3 in Supporting Information S1).

3.2. Network Turnover

The systematic overestimations of Q_{LOSS} and Q_{GAIN} in the 100-m reaches are amplified when results are aggregated along the study segment to predict stream water turnover. The empirical mass recoveries yield higher magnitudes for Q_{LOSS} and Q_{GAIN} in each segment than their extended counterparts (visible as the differences in heights of individual segments within stacked bars of Figure 5a). The result of increased magnitudes is more rapid replacement of upstream waters by downstream inflows for the empirical data in comparison to the extended values. If turnover is overpredicted, then predictions of stream water residence time in the channel will be shorter when compared to extended interpretations, with more outflowing water being attributed to locations closer to the outlet. This effect accumulates along the full length of the stream channel, yielding two related patterns. First, the persistence of upstream waters along the segment is systematically underestimated using empirical data (visible by the preponderance of upstream, "bluer" bars below 0 in Figure 5b). For example, discharge at the outlet from the upstream-most segment is calculated as

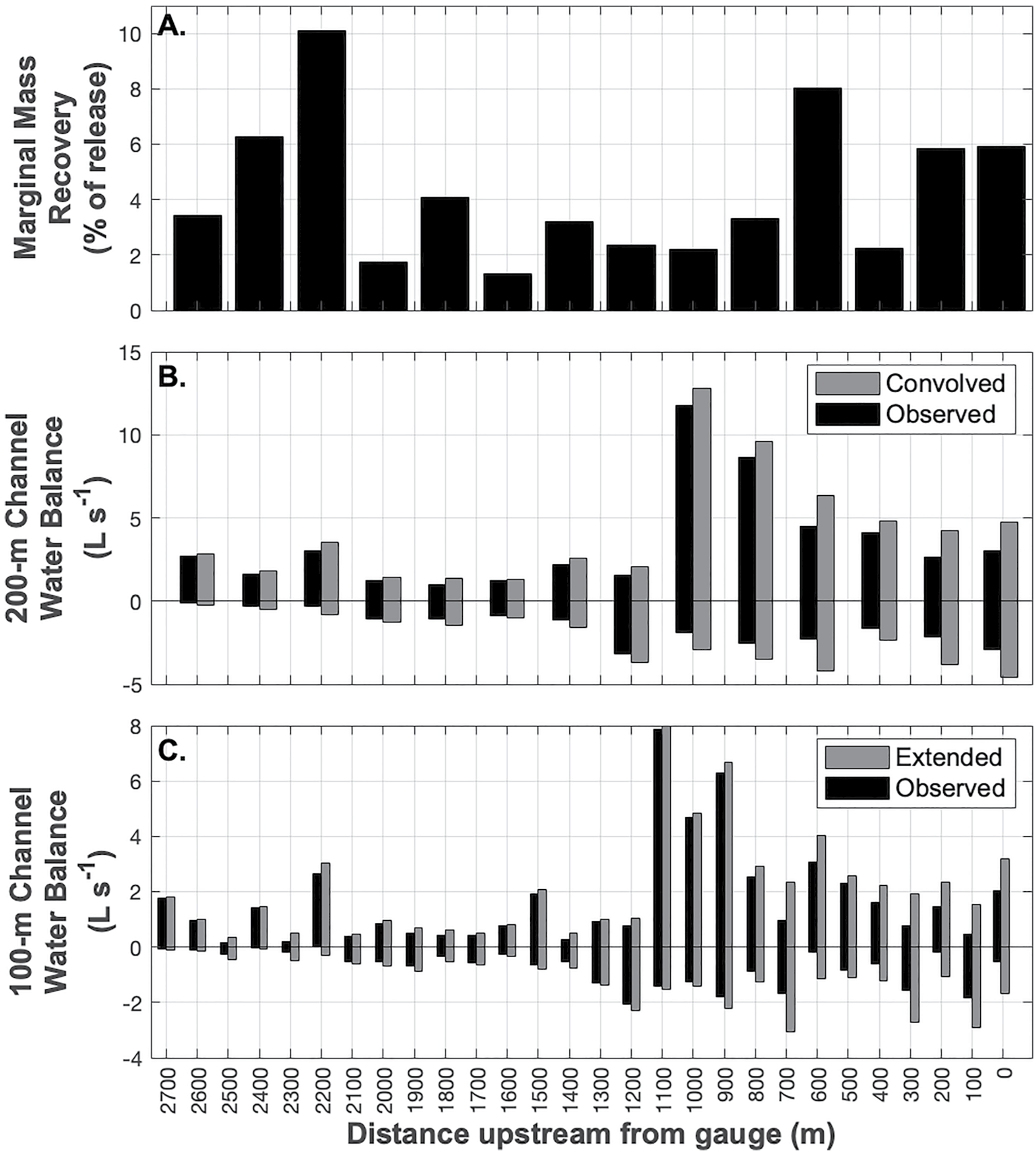

Figure 4. (a) Magnitude of marginal mass recovery for each 200-m reach compared to its component 100-m reaches, expressed as total percent of the tracer released. (b) Gross gains (positive bars) and losses (negative bars) for the observed 200-m experiments and what would be expected based on linear convolution of the underlying 100-m reaches. Convolution of two 100-m segments always yields larger magnitudes of gross gains and losses than are inferred from 200-m studies. (c) Gross gains and losses for 100-m segments using the observed and extended mass balance calculations.

about 0.03 L s^{-1} based on empirical observations, compared to nearly 0.1 L s^{-1} based on extended calculations. At the basin outlet, contributions from the upper 2000-m are underestimated by nearly 50% based on empirical data compared to the extended interpretation. Next, the overpredicted turnover from empirical data requires that downstream contributions are overestimated, yielding a systematic overprediction of the contributions of downstream reaches to the stream water composition (visible by the preponderance of downstream, "yellower" bars above 0 in Figure 5b). For example, at the downstream end of the study segment (right-most bars in Figure 5),

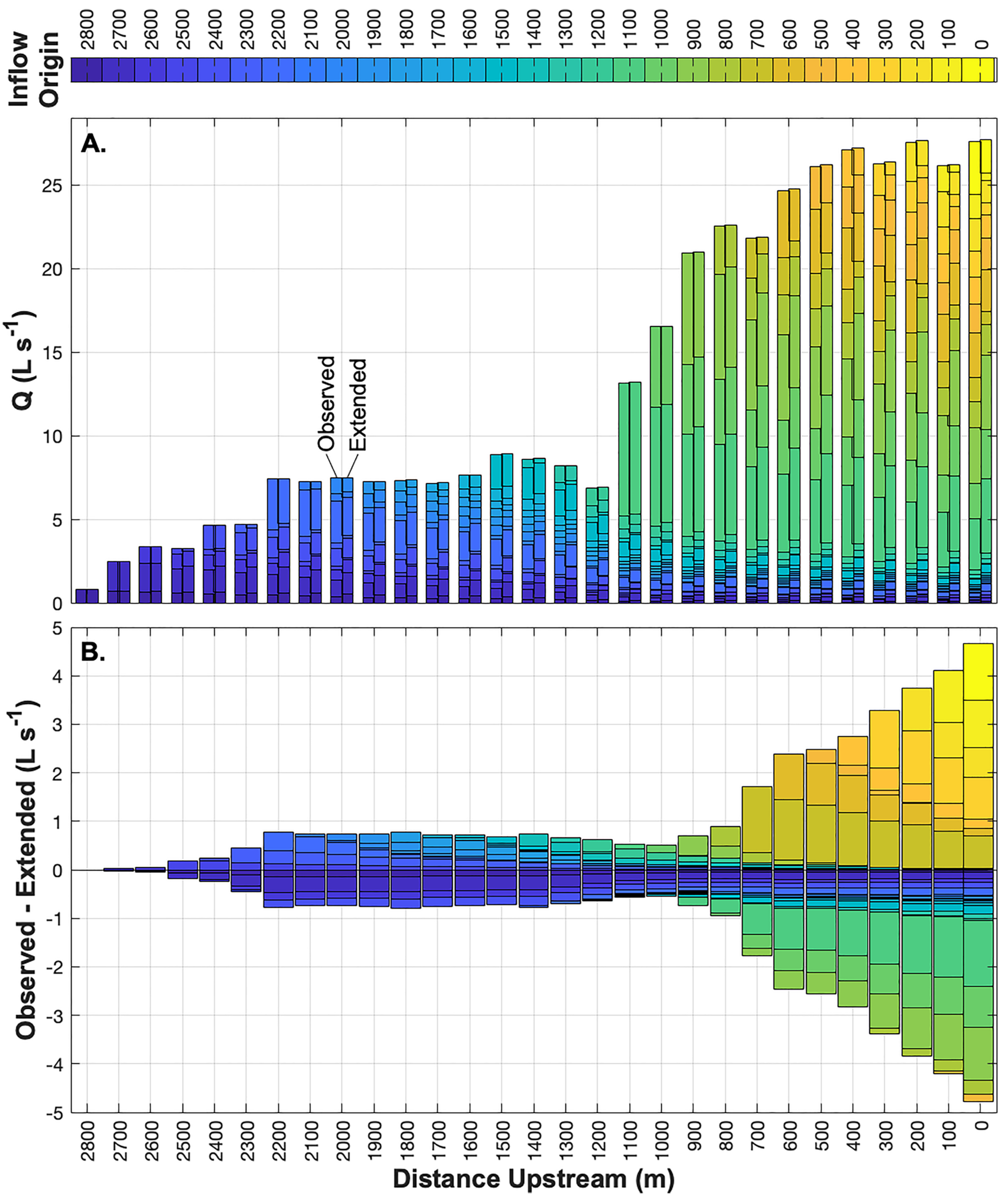

Figure 5. (a) Channel water composition for each segment based on the location of gross gains where water entered the channel, as represented by their color. For each segment, the left stack of bars is derived from the observed mass recoveries, while the right stack includes the marginal mass recoveries. The height of each bar within a "stack" denotes the discharge originating from a given spatial location. While overall patterns are visually similar, differences within the bars show the impact of marginal mass recovery. (b) Differences between the observed and extended mass recoveries for each segment. Values above zero indicate observed values over-estimate contributions, while negative indicate observed values under-estimate contributions to discharge.

inflows from the lower 800-m of the study segment are overestimated at the catchment outlet by about 20%. Thus, while general patterns of turnover are visually similar (Figure 5a), the expected composition of the water in the stream is quite different (Figure 5b) between observed and extended cases.

4. Discussion

4.1. Does Marginal Mass Recovery Change Our Understanding of Reach- and Segment-Scale Channel Water Balance and Network Turnover?

We found the marginal mass recovery (average 4.3% of total tracer) represents an average of 26% of mass that was otherwise lost to unknown fates (i.e., our "black box" in the introduction). In other words, 26% of mass that was previously lost can now be attributed to flowpaths with timescales that are longer than the 100-m WoD but shorter than the 200-m WoD. Thus, not only can the fate of more mass be explained, but it can be assigned to a particular subset of storage timescales. Additionally, the mass that remains lost can now be confidently assigned to timescales longer than the WoD for the 200-m reach. For studies whose primary objective is to characterize the stream transport processes of advection and longitudinal dispersion, marginal mass recovery is likely inconsequential, as such studies have been a cornerstone of research for decades and not apparently suffered due to relatively small mass losses (Fischer, 1979). However, for studies attempting to allocate the age composition of catchment outflows (Harman et al., 2016; Ward, Kurz, et al., 2019; Ward, Wondzell, et al., 2019), marginal mass recovery informs a previously unobserved suite of timescales. We expect that marginal mass recovery will be most important for studies concerned with the fate of water in streams at the reach-scale and longer.

Beyond timescales and ages of water, the flowpaths associated with marginal mass recovery may also impact our interpretations of biogeochemical functioning of study reaches and segments. The biogeochemical importance of flowpaths associated with marginal mass recovery will primarily depend on the timescale of the these flowpaths in comparison to the timescale of the process of interest. Thus, we consider the implications of our findings related to physical processes and timescales for potentially associated biogeochemical functions. For example, consider a rapid process (e.g., with a half-life i.e., 1–2 order of magnitude faster than the WoD). We would expect that reaction would be substantially completed along all flowpaths within the 100-m WoD. In that case, a 4.3% increase in the marginal mass recovery could increase the estimated amount of mass expected to be transformed by the reactive process by as much as 4.3%. Generalizing, for rapid processes, marginal mass recovery will be directly proportional to our inferred amount of transformations occurring in a reach. In this case (where function is biased toward the head of the flowpath), marginal mass recovery will yield a directly proportional increase in realized function per unit of marginal mass recovered. In contrast, consider a typically-slower process in the study reach, such as denitrification (where extensive anaerobic conditions must be present to allow bulk reduction of NO_3^- to occur), following oxygen consumption. Thus, we would expect such a process to occur preferentially at the distal ends of longer residence time flow paths, particularly locations that are longer in transit time than the WoD. By expanding the WoD to include longer flowpaths, we disproportionately add flowpaths that are longer and more likely to have active denitrification to the population of flowpaths we are interpreting. In this case (where function is biased toward longer flowpaths), marginal mass recovery will yield a disproportionately large increase in a function per unit of marginal mass recovered.

Aggregation of errors from reach-scale studies biases segment- and network-scale predictions of their hydrologic turnover and transit times (Figure 5). That we see substantial and variable marginal mass recovery along the study segment suggests that this change is hydrologically relevant, particularly to our ability to extend reach-scale results to estimate turnover for segments or even river networks. One common strategy to upscaling in river corridors is to represent the river as a series of shorter reaches and then route water and solutes through those reaches in series to represent segments and networks (Covino et al., 2011; Gomez-Velez & Harvey, 2014; Gomez-Velez et al., 2015; Kiel & Cardenas, 2014; Mallard et al., 2014). These approaches rely upon the assumption that the processes controlling transport, transformation, or loss do not change as the spatial scale of interest grows. Put another way, we commonly assume the dominant processes measured at one scale can be directly aggregated along the network to represent larger spatial scales without any other processes emerging as important. However, our findings here document that segment-scale results are directly related to the scale of a study that is chosen, consistent with Schmadel et al. (2016). Indeed, we show that even our marginal mass recovery may have a substantial impact on the inferred composition of water along a river segment (Figure 5). Thus, turnover interpreted directly from empirical studies presents a case of maximum plausible turnover, which has the result

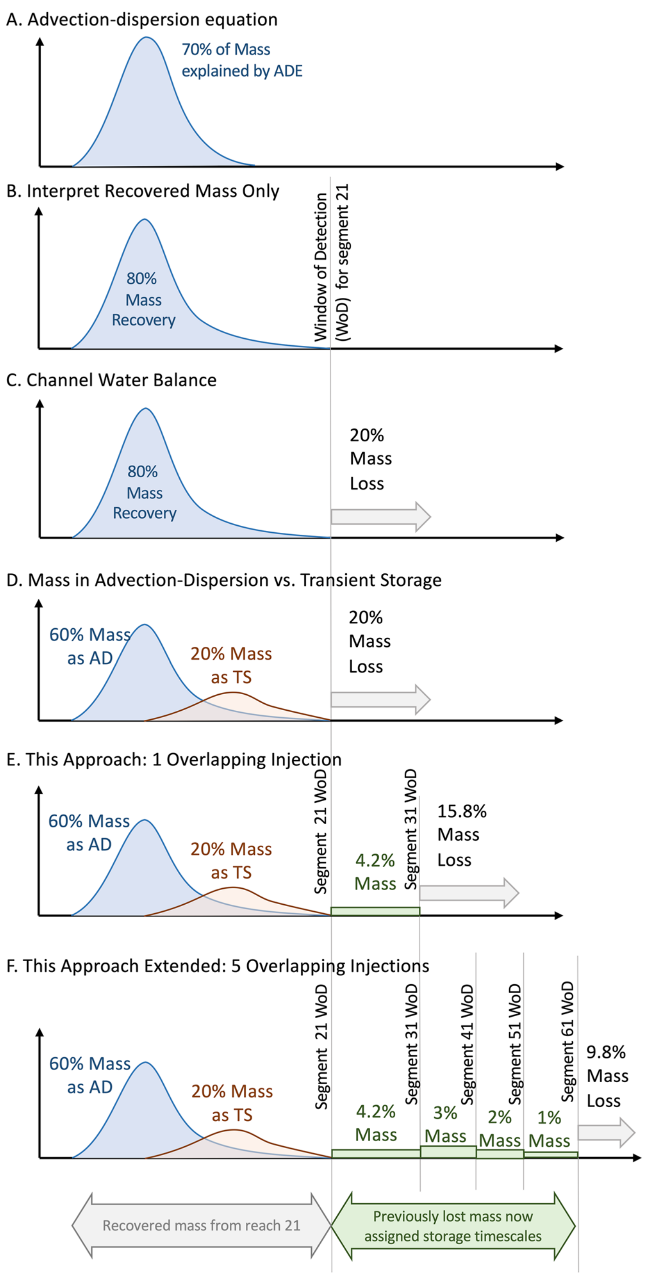

Figure 6. Evolving interpretation of stream solute tracer studies in the past 50 years. Tracer studies were initially used to estimate mixing and dispersion (a), and later transient storage (b). More recent work has extended interpretations to channel water balance (c) and partitioning recovered tracer into fractions with dominant transport by transient storage (d). In this study, we demonstrate manipulation of the window of detection to further assign mass to a range of timescales (e), which could be readily extended with increasingly long reaches and/or sensitivity to different tracers (f). In all cases, the quantitative values provided are intended as illustrative, relative values and not presenting any specific data set.

of minimizing the persistence of upstream contribution and amplifying the proportion of downstream contributions to streamflow. The longer the WoD can be extended, and marginal mass recovery increased, the more persistent upstream inflows will be along a gaining river corridor.

4.2. Past Advances and Future Directions for Stream Solute Tracer Studies

The WoD has fundamentally defined the way solute tracer studies are interpreted for more than 50 years. Early work focused on the recovered solute tracer, including measurement of advective and dispersive processes and the study of mixing zones (e.g., Fischer, 1979; Figure 6a). Comparisons of mass recovery were the basis to assess net gains of stream water via dilution or used to inform losses of reactive compounds (e.g., Newbold et al., 1981). The observed time series (Figure 6b), rather than the total masses, are the basis for studies using the popular transient storage model (Bencala & Walters, 1983; Knapp & Kelleher, 2020; Runkel, 1998), and a host of other modeling approaches (Haggerty & Reeves, 2002; Rathore et al., 2021; Worman et al., 2002) and empirical calculations (Covino et al., 2010). Still, these advances came with the often unstated recognition that the empirical data themselves were subject to limitation (J. W. Harvey et al., 1996; Wagner & Harvey, 1997). The interpretation of tracer mass beyond the WoD has, too, been the subject of inquiry. For example, Payn et al. (2009) implemented a channel water balance, building upon concepts outlined by Harvey et al. (1996). Most recently, partitioning recovered mass into that which is primarily associated with advection and dispersion from that which is primarily associated with transient storage further subdivide recovered mass based on process domain (Mason et al., 2012; Wlostowski et al., 2017; Figure 6d).

In this study we pioneer the interpretation of co-located studies with different WoDs to define and characterize a suite of intermediate timescale flowpaths (empirically in Figure 4a; Figure 5; conceptually in Figure 6e). Using our experimental design, we are now able to divide formerly lost mass into that which is recovered in a marginally longer WoD (M_{marg}). Ultimately, we are empirically documenting another "bin" of timescales and associated solute masses that extend our interpretations in time (Figure 6e). All prior approaches (Figures 6a–6d) are still valid and appropriate, and we admittedly still cannot precisely account for the fate of all unrecovered mass (e.g., we cannot differentiate between all classes of flowpaths in Figure 1). Still, this advance demonstrates that by manipulating the experimental design of a solute tracer study - in this case considering both 100- and 200-m segments - enables interpretation of flowpaths that would not have been considered if only conducting studies at a fixed length. Moreover, this experimental design is not limited to two overlapping segments as we considered here. This approach could be readily extended to consider a series of increasingly longer, overlapping study segments that would enable further resolution at timescales beyond the traditional WoD (Figure 6f) until practical detection limitations are reached for a given solute tracer.

For future studies, especially those that will use empirical data as a basis for estimation of network turnover along segments or networks (after Covino et al., 2011; Mallard et al., 2014), we recommend that assessment of marginal mass recovery is conducted. This could be implemented through multiple overlapping reaches (as demonstrated in our findings), by releasing different masses or types of tracer to extend detection limits for a fixed study segment, or using instruments of varied detection limits in a single reach. Most importantly, we also emphasize here that spatially longer study reaches are expected to capture temporally longer flowpaths, so increased study reach length is recommended as a general strategy. For studies where channel water balance and subsequent network turnover are not the focus, assessment of marginal mass losses may still offer some benefit. For example, while it does not definitively account for the fate of all mass, our approach does generate a realistic range of plausible mass recoveries that provide some estimate beyond the traditional WoD. This allows for a range of plausible segment-scale calculations to be generated, acknowledging the inherent uncertainties in selecting study segments instead of taking the WoD as a fixed limitation that must be "worked around" instead of "worked with".

4.3. Outstanding Uncertainties and Aggregation of Error in Scaling

We contend that marginal mass recovery provides useful reach-scale information about a solute tracer study and how to interpret results, but emphasize here that this strategy does not yield complete understanding of reaches and their exchanges. Consequently, reach-scale studies are incomplete and may not be appropriate for direct convolution to represent longer segments and networks. Marginal mass recovery enables researchers to ask "What would change in my interpretation if my study designs were incrementally different?" and assess the sensitivity of their perceptual models or quantitative predictions to marginal changes at the limits of empirical detection. Still, other sources of error will persist including measurement of tracer masses, equipment calibration, incomplete mixing in streams, and assumptions that a sensor- or sample-based measurement occurs in a representative location in the cross-section of a stream or river. Perhaps most importantly, stream discharge is a critical variable in channel water balance and mass recovery estimates. Error in discharge measurements (due to any of the previously cited potential sources of error if dilution gauging is used) will have a directly proportional impact on inferred mass recovery. Thus, in addition to assessment of marginal mass recovery, we strongly recommend additional care is given to calculation of discharge. This could be realized by making discharge measurements independently of the tracer (e.g., via velocity gauging or co-location a station with an established stream gauge), building a stage-discharge relationship from several replication dilution gauging experiments, using multiple in-stream sensors to validate complete mixing (e.g., Clow & Fleming, 2008), or otherwise assessing uncertainty in discharge and propagating that through calculations (Emmanuelson et al., 2022; Ward, Wondzell, et al., 2019). Any error in study of an individual segment may propagate through the analysis, and small errors could be amplified in the convolution of reaches to represent study segments. We also note that our analyses assume steady-state discharge conditions; unsteady discharge would further complicate analysis and meaningful interpretation of empirical results.

Beyond error at the reach scale, the analysis of network turnover highlights the potentially compounding and propagating of error that is possible as we represent segments and networks as a series of reaches operating in serial (as in Covino et al., 2011; Gomez-Velez & Harvey, 2014; J. Harvey et al., 2019; Kiel & Cardenas, 2014; Figure 6). Indeed, this representation of segments requires several assumptions that are not always explicitly stated nor justified. First, the approach requires that the reach-scale experiments are, themselves, an appropriate scale to characterize the most important processes. In the case of hyporheic exchange, one practical consequence is assuming that unmeasured flowpaths beyond the WoD are unimportant. Next, the approach requires that the processes that are integrated by the recovered tracer at the reach-scale are characterized by the empirical data. Put another way, the reach itself must be a representative sampling of the processes that are important. This has been assumed by fixing study reach lengths (as in this study and Schmadel et al., 2016), advective timescales (e.g., Ward, Zarnetske, et al., 2019), establishing a standardized length-scale (Runkel, 2002), or assuming that a scale established by one discipline will be relevant for another (e.g., 20 wetted channel widths as a reach-scale from geomorphologists as a basis for planning solute tracer studies; Ward, Zarnetske, et al., 2019, Ward, Wondzell, et al., 2019). To our knowledge, none of these assumptions has been explicitly tested in the field for solute tracer studies. Finally, this approach assumes that no new controls will emerge as important as spatial scales are increased.

5. Conclusions

Our overarching goal was to identify if and how marginally extended the window of detection, and thereby extended empirical mass recovery to a broader suite of flowpaths, would change our understanding of reach- and segment-scale transport in river corridors. We found that shorter (100-m) reaches did not systematically bias toward more or less mass recovery than the 200-m reaches they were located within. Marginal mass recovery was able to explain an average of about 26% of lost tracer mass, representing an average of 4.3% of total solute tracer mass (range 1.3%–10.1%) across our replicates. This change in mass recovery was important, as we found representing a 200-m reach as a series of 2 × 100-m reaches systematically underestimate mass recovery. Consequently, studies without marginal mass recovery overestimated magnitudes of gross gains and losses in the marginally longer 200-m reaches in all cases. Moreover, this bias was amplified when we represented segments as a series of reaches, leading to interpretations that underestimated the persistence of distal segments and overestimated the importance of gains occurring near the catchment outlet.

Ultimately, some amount of solute mass loss to unknown fates is to be expected in any solute tracer study given detection limits and complex, multi-scale flowpath networks. Thus, we suggest that researchers embrace the window of detection, taking advantage of experimental design to assess marginal mass recovery. This provides context for interpretation of empirical data, yielding a quantitative basis for assessment of uncertainty associated with detection limits. Moreover, if tracers, sensitivities, or experimental designs are planned appropriately, marginal mass recovery could be used to systematically probe flowpaths with longer duration (e.g., Figure 6f), informing transport at previously unobserved timescales.

Finally, the use of reach-scale understanding as a basis for representation of segments (as a series of reaches) or network (as a series of segments) is being used as one basis to make predictions at large spatial scales (e.g., Covino et al., 2011; Gomez-Velez et al., 2015; Kiel & Cardenas, 2014). However, we encourage caution in aggregating reaches to represent segments and network, as this implicitly assumes (a) that reach-scale results are complete in their representation of timescales and processes; (b) reach-scale results appropriately integrate all smaller-scale controls relevant for the process(es) of interest; and (c) no new controls emerge at larger spatial scales that would not be apparent in reach-scale studies. On balance, we expect that short reach-scale studies will truncate more of the true, underlying transit time distribution and exacerbate errors associated with scaling.

Data Availability Statement

Stream solute tracer experiments including solute slug masses, release times and locations, and the observed in-stream timeseries are available in Payn and Ward (2022).

Acknowledgments

The initial data collection was research was supported by collaborative NSF awards EAR 0337650 and EAR 0530873. The authors thank the Tenderfoot Creek Experimental Forest and the U.S. Department of Agriculture for support of field research at the site. The authors thank Ken Bencala for input on early versions of this study and continued mentoring. Ward led the data analysis and writing of this manuscript, with input and support from all coauthors. Ward was support in part by Department of Energy awards DE-SC000022 and DE-SC0019377. Ward's time was supported in part by NSF Award EAR 1652293, the Burnell and Barbara Fischer fellowship from Indiana University, sabbatical support from J. Selker and Oregon State University, and the Fulbright – University of Birmingham Scholar program. Any views or opinions expressed in this study are those of the authors and not positions of their employers.

References

Alexander, R. B., Böhlke, J. K., Boyer, E. W., David, M. B., Harvey, J. W., Mulholland, P. J., et al. (2009). Dynamic modeling of nitrogen losses in river networks unravels the coupled effects of hydrological and biogeochemical processes. *Biogeochemistry*, *93*(1–2), 91–116. https://doi.org/10.1007/S10533-008-9274-8/FIGURES/7

Bencala, K. E. (1983). Simulation of solute transport in a mountain pool-and-riffle stream with a kinetic mass transfer model for sorption. *Water Resources Research*, *19*(3), 732–738. https://doi.org/10.1029/WR019i003p00732

Bencala, K. E., Kennedy, V. C., Zellweger, G. W., Jackman, A. P., & Avanzino, R. J. (1984). An experimental analysis of cation and anion transport. *Water Resources Research*, *20*(12), 1797–1803. https://doi.org/10.1029/wr020i012p01797

Bencala, K. E., & Walters, R. A. (1983). Simulation of solute transport in a mountain pool-and-riffle stream: A transient storage model. *Water Resources Research*, *19*(3), 718–724. https://doi.org/10.1029/WR019i003p00718

Briggs, M. A., Gooseff, M. N., Arp, C. D., & Baker, M. A. (2009). A method for estimating surface transient storage parameters for streams with concurrent hyporheic storage. *Water Resources Research*, *45*(4), W00D27. https://doi.org/10.1029/2008wr006959

Cirpka, O. A., Fienen, M. N., Hofer, M., Hoehn, E., Tessarini, A., Kipfer, R., & Kitanidis, P. K. (2007). Analyzing bank filtration by deconvoluting time series of electric conductivity. *Ground Water*, *45*(3), 318–328. https://doi.org/10.1111/j.1745-6584.2006.00293.x

Clow, D. W., & Fleming, A. C. (2008). Tracer gauge: An automated dye dilution gauging system for ice-affected streams. *Water Resources Research*, *44*(12), W12441. https://doi.org/10.1029/2008WR007090

Covino, T. P., McGlynn, B. L., & Mallard, J. (2011). Stream-groundwater exchange and hydrologic turnover at the network scale. *Water Resources Research*, *47*(12), W12521. https://doi.org/10.1029/2011wr010942

Covino, T. P., McGlynn, B. L., & McNamara, R. A. (2010). Tracer Additions for Spiraling Curve Characterization (TASCC): Quantifying stream nutrient uptake kinetics from ambient to saturation. *Limnology and Oceanography: Methods*, *8*(9), 484–498. https://doi.org/10.4319/lom.2010.8.484

Drummond, J. D., Covino, T. P., Aubeneau, a. F., Leong, D., Patil, S., Schumer, R., & Packman, A. I. (2012). Effects of solute breakthrough curve tail truncation on residence time estimates: A synthesis of solute tracer injection studies. *Journal of Geophysical Research*, *117*(3), 1–11. https://doi.org/10.1029/2012JG002019

Emmanuelson, K., Covino, T. P., Ward, A. S., Dorley, J., & Gooseff, M. N. (2022). Conservative solute transport processes and associated transient storage mechanisms: Comparing streams with contrasting channel morphologies, land use, and land cover. *Hydrological Processes*, *36*(4), e14654. https://doi.org/10.1002/hyp.14564

Fischer, H. B. (1979). *Mixing in inland and coastal waters*. Academic Press.

Frissell, C. A., Liss, W. J., Warren, C. E., & Hurley, M. D. (1986). A hierarchical framework for stream habitat classification: Viewing streams in a watershed context. *Environmental Management*, *10*(2), 199–214. https://doi.org/10.1007/bf01867358

Fuller, C. C., & Harvey, J. W. (2000). Reactive uptake of trace metals in the hyporheic zone of a mining-contaminated stream, Pinal Creek, Arizona. *Environmental Science & Technology*, *34*(7), 1150–1155. https://doi.org/10.1021/es990714d

Gomez-Velez, J. D., & Harvey, J. W. (2014). A hydrogeomorphic river network model predicts where and why hyporheic exchange is important in large basins. *Geophysical Research Letters*, *41*(18), 6403–6412. https://doi.org/10.1002/2014GL061099

Gomez-Velez, J. D., Harvey, J. W., Cardenas, M. B., & Kiel, B. (2015). Denitrification in the Mississippi River network controlled by flow through river bedforms. *Nature Geoscience*, *8*, 1–8. https://doi.org/10.1038/ngeo2567

Gooseff, M. N., McKnight, D. M., Runkel, R. L., & Vaughan, B. H. (2003). Determining long time-scale hyporheic zone flow paths in Antarctic streams. *Hydrological Processes*, *17*(9), 1691–1710. https://doi.org/10.1002/hyp.1210

Guillet, G., Knapp, J. L. A., Merel, S., Cirpka, O. A., Grathwohl, P., Zwiener, C., & Schwientek, M. (2019). Fate of wastewater contaminants in rivers: Using conservative-tracer based transfer functions to assess reactive transport. *Science of the Total Environment*, *656*, 1250–1260. https://doi.org/10.1016/J.SCITOTENV.2018.11.379

Haggerty, R., & Reeves, P. (2002). STAMMT-L version 1.0 user's manual. Sandia national laboratories [ERMS# 520308] (pp. 1–76).

Haggerty, R., Wondzell, S. M., & Johnson, M. A. (2002). Power-law residence time distribution in the hyporheic zone of a 2nd-order mountain stream. *Geophysical Research Letters*, *29*(13), 1640. https://doi.org/10.1029/2002gl014743

Harman, C. J., Ward, A. S., & Ball, A. (2016). How does reach-scale stream-hyporheic transport vary with discharge? Insights fromrSAS analysis of sequential tracer injections in a headwater mountain stream. *Water Resources Research*, *52*(9), 7130–7150. https://doi.org/10.1002/2016WR018832.Received

Harvey, J., Gomez-Velez, J., Schmadel, N. M., Scott, D., Boyer, E. W., Alexander, R. B., et al. (2019). How hydrologic connectivity regulates water quality in river corridors. *Journal of the American Water Resources Association*, *55*(2), 369–381. https://doi.org/10.1111/1752-1688.12691

Harvey, J. W., & Fuller, C. C. (1998). Effect of enhanced manganese oxidation in the hyporheic zone on basin-scale geochemical mass balance. *Water Resources Research*, *34*(4), 623–636. https://doi.org/10.1029/97wr03606

Harvey, J. W., & Wagner, B. J. (2000). Quantifying hydrologic interactions between streams and their subsurface hyporheic zones. In J. B. Jones & P. J. Mulholland (Eds.), *Streams and ground waters* (pp. 3–44).

Harvey, J. W., Wagner, B. J., & Bencala, K. E. (1996). Evaluating the reliability of the stream tracer approach to characterize stream-subsurface water exchange. *Water Resources Research*, *32*(8), 2441–2451. https://doi.org/10.1029/96wr01268

Herzog, S. P., Ward, A. S., & Wondzell, S. M. (2019). Multiscale feature-feature interactions control patterns of hyporheic exchange in a simulated headwater mountain stream. *Water Resources Research*, *55*, (12), 1–17. https://doi.org/10.1029/2019WR025763

Jackman, A. P., Walters, R. A., & Kennedy, V. C. (1984). Transport and concentration controls for chloride, strontium, potassium and lead in Uvas Creek, a small cobble-bed stream in Santa Clara County, California, U.S.A.: 2. Mathematical modeling. *Journal of Hydrology*, *75*(1–4), 111–141. https://doi.org/10.1016/0022-1694(84)90047-7

Jackson, T. R., Haggerty, R., Apte, S. V., Coleman, A., & Drost, K. J. (2012). Defining and measuring the mean residence time of lateral surface transient storage zones in small streams. *Water Resources Research*, *48*(10), 1–20. https://doi.org/10.1029/2012WR012096

Jackson, T. R., Haggerty, R., Apte, S. V., & O'Connor, B. L. (2013). A mean residence time relationship for lateral cavities in gravel-bed rivers and streams: Incorporating streambed roughness and cavity shape. *Water Resources Research*, *49*(6), 3642–3650. https://doi.org/10.1002/wrcr.20272

Karwan, D. L., & Saiers, J. E. (2009). Influences of seasonal flow regime on the fate and transport of fine particles and a dissolved solute in a New England stream. *Water Resources Research*, *45*(11), W11423. https://doi.org/10.1029/2009wr008077

Keefe, S. H., Barber, L. B., Runkel, R. L., Ryan, J. N., Mcknight, D. M., Wass, R. D., et al. (2004). Conservative and reactive solute transport in constructed wetlands. *Water Resources Research*, *40*(1), 1201. https://doi.org/10.1029/2003WR002130

Kelleher, C. A., Wagener, T., McGlynn, B. L., Ward, A. S., Gooseff, M. N., & Payn, R. A. (2013). Identifiability of transient storage model parameters along a mountain stream. *Water Resources Research*, *49*(9), 5290–5306. https://doi.org/10.1002/wrcr.20413

Kiel, B., & Cardenas, M. (2014). Lateral hyporheic exchange throughout the Mississippi River network. *Nature Geoscience*, *7*, 413–417. https://doi.org/10.1038/ngeo2157

Klocker, C. A., Kaushal, S. S., Groffman, P. M., Mayer, P. M., & Morgan, R. P. (2009). Nitrogen uptake and denitrification in restored and unrestored streams in urban Maryland, USA. *Aquatic Sciences-Research Across Boundaries*, *71*(4), 411–424. https://doi.org/10.1007/s00027-009-0118-y

Knapp, J. L. A., & Kelleher, C. (2020). A perspective on the future of transient storage modeling: Let's stop chasing our tails. *Water Resources Research*, *56*(3), e2019WR026257. https://doi.org/10.1029/2019WR026257

Knust, A. E., Warwocl, J. J., & Warwick, J. J. (2009). Using a fluctuating tracer to estimate hyporheic exchange in restored and unrestored reaches of the Truckee River, Nevada, USA. *Hydrological Processes*, *23*(8), 1119–1130. https://doi.org/10.1002/hyp.7218

Lamontagne, S., & Cook, P. G. (2007). Estimation of hyporheic water residence time in situ using 222Rn disequilibrium. *Limnology and Oceanography: Methods*, *5*(11), 407–416. https://doi.org/10.4319/LOM.2007.5.407

Lange, J., Schuetz, T., Gregoire, C., Elsässer, D., Schulz, R., Passeport, E., & Tournebize, J. (2011). Multi-tracer experiments to characterise contaminant mitigation capacities for different types of artificial wetlands. *International Journal of Environmental Analytical Chemistry*, *91*(7–8), 768–785. https://doi.org/10.1080/03067319.2010.525635

Larson, L. N., Fitzgerald, M., Singha, K., Gooseff, M. N., Macalady, J. L., & Burgos, W. (2013). Hydrogeochemical niches associated with hyporheic exchange beneath an acid mine drainage-contaminated stream. *Journal of Hydrology*, *501*, 163–174. https://doi.org/10.1016/j.jhydrol.2013.08.007

Mallard, J., McGlynn, B. L., & Covino, T. P. (2014). Lateral inflows, stream-groundwater exchange, and network geometry influence streamwater composition. *Water Resources Research*, *50*(6), 4603–4623. https://doi.org/10.1002/2013WR014222.Received

Mason, S. J. K., McGlynn, B. L., & Poole, G. C. (2012). Hydrologic response to channel reconfiguration on Silver Bow Creek, Montana. *Journal of Hydrology*, *438–439*, 125–136. https://doi.org/10.1016/j.jhydrol.2012.03.010

Mulholland, P. J., Helton, A. M., Poole, G. C., Hall, R. O., Hamilton, S. K., Peterson, B. J., et al. (2008). Stream denitrification across biomes and its response to anthropogenic nitrate loading. *Nature*, *452*(7184), 202–205. https://doi.org/10.1038/nature06686

Newbold, J. D., Elwood, J. W., O'Neill, R. V., & Van Winkle, W. (1981). Measuring Nutrient Spiraling in Streams. *Canadian Geotechnical Journal*, *38*(7), 860–863. https://doi.org/10.1139/f81-114

Ninnemann, J. J. (2005). *A study of hyporheic characteristics along a longitudinal profile of Lookout Creek, Oregon*. Oregon State University. https://doi.org/10.1017/CBO9781107415324.004

Patil, S., Covino, T. P., Packman, A. I., McGlynn, B. L., Drummond, J. D., Payn, R. A., & Schumer, R. (2013). Intrastream variability in solute transport: Hydrologic and geomorphic controls on solute retention. *Journal of Geophysical Research: Earth Surface*, *118*(2), 413–422. https://doi.org/10.1029/2012JF002455

Payn, R. A., Gooseff, M. N., McGlynn, B. L., Bencala, K. E., & Wondzell, S. M. (2009). Channel water balance and exchange with subsurface flow along a mountain headwater stream in Montana, United States. *Water Resources Research*, *45*(11), W11427. https://doi.org/10.1029/2008wr007644

Payn, R. A., & Ward, A. S. (2022). Solute tracer timeseries, Stringer Creek, 2005 and 2006 [Dataset]. HydroShare. https://doi.org/10.4211/hs.efb41192ddbd4785a2b0ef00bf5e7c62

Rathore, S. S., Jan, A., Coon, E. T., & Painter, S. L. (2021). On the reliability of parameter inferences in a multiscale model for transport in stream corridors. *Water Resources Research*, *57*(5), e2020WR028908. https://doi.org/10.1029/2020WR028908

Runkel, R. L. (1998). *One-dimensional Transport with Inflow and Storage (OTIS): A solute transport model for streams and rivers. Director*. US Department of the Interior, US Geological Survey. Information Services [distributor]. https://doi.org/10.3133/wri984018

Runkel, R. L. (2002). A new metric for determining the importance of transient storage. *Journal of the North American Benthological Society*, *21*(4), 529–543. https://doi.org/10.2307/1468428

Schmadel, N. M., Nielson, B. M., & Kasahara, T. (2013). Deducing the spatial variability of exchange within a longitudinal channel water balance. *Hydrological Processes*, *28*(7), 3088–3103. https://doi.org/10.1002/hyp.9854

Schmadel, N. M., Ward, A. S., Kurz, M. J., Fleckenstein, J. H., Zarnetske, J. P., Knapp, J. L. A., et al. (2016). Stream solute tracer timescales changing with discharge and reach length confound process interpretation. *Water Resources Research*, *52*(4), 3227–3245. https://doi.org/10.1002/2015WR018062.Received

Tank, J. L., Rosi-Marshall, E. J., Baker, M. A., & Hall, R. O. (2008). Are rivers just big streams? A pulse method to quantify nitrogen demand in a large river. *Ecology*, *89*(10), 2935–2945. https://doi.org/10.1890/07-1315.1

Toth, J. (1962). A theory of groundwater motion in small drainage basins in central Alberta, Canada. *Journal of Geophysical Research*, *67*(11), 4375–4387. https://doi.org/10.1029/jz067i011p04375

Tóth, J. (1963). A theoretical analysis of groundwater flow in small drainage basins. *Journal of Geophysical Research*, *68*(16), 4795–4812. https://doi.org/10.1029/JZ068i016p04795

Wagner, B. J., & Harvey, J. W. (1997). Experimental design for estimating parameters of rate-limited mass transfer: Analysis of stream tracer studies. *Water Resources Research*, *33*(7), 1731–1741. https://doi.org/10.1029/97wr01067

Ward, A. S., Fitzgerald, M., Gooseff, M. N., Voltz, T. J., Binley, A. M., & Singha, K. (2012). Hydrologic and geomorphic controls on hyporheic exchange during base flow recession in a headwater mountain stream. *Water Resources Research*, *48*(4), W04513. https://doi.org/10.1029/2011wr011461

Ward, A. S., Gooseff, M. N., Voltz, T. J., Fitzgerald, M., Singha, K., & Zarnetske, J. P. (2013). How does rapidly changing discharge during storm events affect transient storage and channel water balance in a headwater mountain stream? *Water Resources Research*, *49*(9), 5473–5486. https://doi.org/10.1002/wrcr.20434

Ward, A. S., Kelleher, C. A., Mason, S. J. K., Wagener, T., McIntyre, N., McGlynn, B., et al. (2016). A software tool to assess uncertainty in transient-storage model parameters using Monte Carlo simulations. *Freshwater Science*, *36*(1), 195–217. https://doi.org/10.1086/690444

Ward, A. S., Kurz, M. J., Schmadel, N. M., Knapp, J. L. A., Blaen, P. J., Harman, C. J., et al. (2019). Solute transport and transformation in an intermittent, headwater mountain stream with diurnal discharge fluctuations. *Water (Switzerland)*, *11*(11), 2208. https://doi.org/10.3390/w11112208

Ward, A. S., Morgan, J. A., White, J. R., & Royer, T. V. (2018). Streambed restoration to remove fine sediment alters reach-scale transient storage in a low-gradient 5 th order river, Indiana, USA. *Hydrological Processes*, *32*, (12), 1–15. https://doi.org/10.1002/hyp.11518

Ward, A. S., Payn, R. A., Gooseff, M. N., McGlynn, B. L., Bencala, K. E., Kelleher, C. A., et al. (2013). Variations in surface water-ground water interactions along a headwater mountain stream: Comparisons between transient storage and water balance analyses. *Water Resources Research*, *49*(6), 3359–3374. https://doi.org/10.1002/wrcr.20148

Ward, A. S., Wondzell, S. M., Schmadel, N. M., Herzog, S., Zarnetske, J. P., Baranov, V., et al. (2019). Spatial and temporal variation in river corridor exchange across a 5th order mountain stream network. *Hydrology and Earth System Sciences Discussions*, *23*, 5199–5225. https://doi.org/10.5194/hess-2019-108

Ward, A. S., Zarnetske, J. P., Baranov, V., Blaen, P. J., Brekenfeld, N., Chu, R., et al. (2019). Co-located contemporaneous mapping of morphological, hydrological, chemical, and biological conditions in a 5th-order mountain stream network, Oregon, USA. *Earth System Science Data*, *11*(4), 1567–1581. https://doi.org/10.5194/essd-11-1567-2019

Wlostowski, A. N., Gooseff, M. N., Bowden, W. B., & Wollheim, W. M. (2017). Stream tracer breakthrough curve decomposition into mass fractions: A simple framework to analyze and compare conservative solute transport processes. *Limnology and Oceanography: Methods*, *15*(2), 140–153. https://doi.org/10.1002/lom3.10148

Workshop, S. S. (1990). Concepts and methods for assessing solute dynamics in stream ecosystems. *Journal of the North American Benthological Society*, *9*(2), 95–119. https://doi.org/10.2307/1467445

Worman, A., Packman, A. I., & Jonsson, K. (2002). Effect of flow-induced exchange in hyporheic zones on longitudinal transport of solutes in streams and rivers Ha. *Water Resources Research*, *38*(1), 2-1–2-15. https://doi.org/10.1029/2001wr000769

Worman, A., & Wachniew, P. (2007). Reach scale and evaluation methods as limitations for transient storage properties in streams and rivers. *Water Resources Research*, *43*(10), W10405. https://doi.org/10.1029/2006wr005808